Performance Evaluation 167 (2025) 102460

Contents lists available at ScienceDirect

Performance Evaluation

journal homepage: www.elsevier.com/locate/peva

Enabling grant-free multiple access through Successive Interference Cancellation

Asmad Bin Abdul Razzaque *, Andrea Baiocchi

Sapienza University of Rome, Via Eudossiana, 18, Rome, 00184, Italy

ARTICLE INFO

Keywords:
Grant-free multiple access
Successive interference cancellation
Slotted ALOHA
CSMA
Non-Orthogonal Multiple Access

ABSTRACT

Internet of Things (IoT) is stirring a surge of interest in effective methods for sharing communication channels, with nodes transmitting sporadic, short messages. These messages are often related to control systems that collect sensor data to drive process actuation, such as in industries, autonomous vehicles, and environmental control. Traditional approaches that dominate wireless and cellular communications prove most effective when dealing with a limited number of concurrently active nodes, sending relatively large volumes of data. We address a different scenario where numerous nodes generate and transmit short messages according to non-periodic schedules. In such cases, random multiple access becomes the typical approach for sharing the communication channel. We propose a general modeling framework that enables the investigation of the impact of Successive Interference Cancellation (SIC) on two of the main random access paradigms, namely Slotted ALOHA (SA) and Carrier-Sense Multiple Access (CSMA). The key varying parameter is the target Signal to Interference plus Noise Ratio (SINR) at the receiver, directly tied to the spectral efficiency of the adopted coding and modulation scheme. Two different regimes are highlighted that bring the system to work at relative maxima of the sum-rate. We further investigate the impact of different transmission power settings and imperfect interference cancellation. Leveraging on the insight gained in the saturated node scenario, an adaptive algorithm is defined for the dynamic case, where the number of backlogged nodes varies over time. The numerical results provide evidence of a significant potential for grant-free multiple access, calling for practical algorithms to translate this promise into feasible realizations.

1. Introduction

Recent evolution of massive multiple access is driven by distinctive service characteristics: sporadic traffic, small payload, low power, latency constraints [1]. All these are also the key characteristics of massive IoT applications [2]. The emphasis on a large population of nodes, each generating a small flow of data in a generally hard-to-predict way, poses challenges that are not adequately met by the current solutions in cellular and wireless communication standards. Hence, new concepts are required to address the challenges of highly dynamic and sporadic traffic, quality of services, and Radio Access Network (RAN) congestion, especially for Machine-to-Machine (M2M) communications [1,3,4].

The traditional response to deal with sporadic traffic generated by a possibly time-varying population of devices consists of Random Access (RA) protocols. SA is a classic RA technique in which users send their bursts within slots in a distributed way. The average normalized throughput of classic SA cannot exceed the $1/e$ limit due to collisions among simultaneous transmissions and

* Corresponding author.
E-mail addresses: asmadbin.razzaque@uniroma1.it (A.B.A. Razzaque), andrea.baiocchi@uniroma1.it (A. Baiocchi).

https://doi.org/10.1016/j.peva.2024.102460

Available online 1 December 2024

idle slots. CSMA is known to break this limit, as long as channel sensing works. It has been widely adopted in wired and wireless Local Area Networks (LANs), e.g., it is the core algorithm for the distributed coordination function of WiFi at least up to IEEE 802.11ac and still plays a major role in the last WiFi version, IEEE 802.11ax.

Improving the performance of classic random access protocols for next-generation wireless systems requires advanced physical layer functions yielding effective Multi-Packet Reception (MPR). This essentially leads us to grant-free random access protocols, in which based on MPR functionality every device is allowed to transmit data to the Base Station (BS) without waiting for the permission [5]. Grant-free random multiple access targets the issue of massive connectivity, with the help of advanced physical layer receiver capabilities [6]. Massive connectivity is the major requirement for future communication systems. As an example, 6G requirements encompass a device density of 10 million/km^2 [7].

A key enabling factor towards grant-free multiple access is Non-Orthogonal Multiple Access (NOMA), which allows multiple users to transmit by using the same resources. NOMA utilizes advanced signal processing techniques like SIC, to enable MPR at the receiver. The literature in this domain has explored the integration of MPR and NOMA into various random access protocols, sparking discussions about their benefits and implications [8–16].

In the quest for efficient wireless systems, a significant gap remains in understanding the interaction between multiple access protocols and advanced physical layer functions. While existing studies have touched upon the promise of these techniques [17,18], a comprehensive analysis of the interplay between Medium Access Control (MAC) and Physical (PHY) layers is yet to be understood in detail. This paper aims to contribute such understanding, by providing a general modeling framework of RA with SIC capable physical layer. The presented results extend the analysis of our previous work [19]. Extensions are along two main lines. First, besides sum-rate, in the present work we look into mean consumed energy per delivered packet and mean AoI. Second, we analyze in depth the stability of an adaptive, grant-free algorithm with a varying number of active nodes.

Summing up, we provide the following main original contributions:

- We highlight the sensitivity of the already identified two regimes in [20] with respect to number of transmitting nodes: (i) high spectral efficiency, where CSMA outperforms SA in terms of sum-rate, and SIC gives little contribution to system performance; and (ii) low spectral efficiency, where the effect of MAC protocol is marginal, and performance is dominated by SIC.
- We identify the impact of imperfect interference cancellation, showing that even 10% residual interference can significantly impair the maximum achievable sum-rate.
- We highlight the impact of different transmission power setting schemes on achievable performance in terms of sum-rate, mean consumed energy per delivered packet and mean AoI.
- We exploit the insights gained in the analysis of sum-rate to define an adaptive algorithms to adjust key system parameters as the number of backlogged nodes varies. The adaptive algorithm guarantees the stability of the channel while maximizing the long-term average sum-rate.

The rest of the paper is organized as follows. Related work is discussed in Section 2. Section 3 summarizes the modeling approach and the main assumptions. Expressions of considered performance metrics are introduced in Section 4. Numerical results are provided in Section 5. Section 6 presents the dynamic optimization of sum-rate. Conclusions are drawn in Section 7, including future work directions.

2. Related work

An extensive literature has been growing on new multiple access techniques [8–10], especially NOMA, to support a massive number of devices, that send infrequent, short data packets, which cannot be effectively accommodated using orthogonal resources [12,21,22]. Hence, emerging multiple access techniques are driving a paradigm shift from grant-based random access to grant-free transmission [23,24]. This shift allows users to transmit data at any time without scheduling a request, leveraging the potential of NOMA for massive machine-type communication [12,24,25]. A powerful approach to realize grant-free multiple access is offered by SIC [26,27].

The potential throughput improvement carried over by MPR capabilities enhancing classic multiple random access protocols, e.g., Slotted ALOHA, has been highlighted by several works, e.g., [28–31]. A notable throughput improvement with respect to Slotted ALOHA involves transmitting each packet multiple times in different time slots, an approach known as Irregular Repetition Slotted ALOHA (IRSA) as proposed in [32]. Our focus is more towards understanding the role of SIC in each slot, with no multiple transmission of a packet in different slots. More recently, the impact of MPR, and specifically SIC based, multiple access protocols has been examined with respect to metrics such as energy consumption and AoI [33,34].

Two SIC receiver models are analyzed in [17]: ordered SIC and unordered SIC. The main contribution involves the understanding of implications of SIC receivers and their comparison with the capture model, along with shedding light on rate losses due to uncoordinated transmissions in SA networks [17]. A few additional works delve into power allocation strategies within random access protocols [15,16]. The evolving landscape is evident as studies explore SIC's network-level impacts [13,14,18], prompting a reconsideration of upper-layer protocols for IoT scenarios. Furthermore, in [13,35], the performance of grant-free access is investigated by incorporating ALOHA and Slotted ALOHA protocols with Power-domain Non-Orthogonal Multiple Access (PD-NOMA). PD-NOMA regulates transmission power levels, thus allowing SIC to work effectively [36].

A SIC-aware based scheduling algorithm is presented in [37], to extract the most gains from SIC. This work also highlighted the extent of throughput gains possible with SIC from a MAC layer perspective along with the scenarios where such gains are worth pursuing. The relative gains from SIC can be maximized when the power level of two transmitters is adjusted in such a way that

the feasible bit-rate is equal for both transmissions [37]. Most of these studies are primarily focused towards PHY layer or the MAC layer, and the existence of different regimes in sum-rate is not identified in any of these in terms of MAC, PHY layer perspective. Here we present an in-depth investigation of achievable sum-rate based on a general modeling approach introduced in our previous work [20], where PHY and MAC are jointly analyzed.

Adaptive random access protocols have gained great attention from researchers recently, to improve the system capacity and latency, in highly dynamic and sporadic traffic environments [38–40].

A grant-free based adaptive parameter system is studied in [38] for 5G systems to address Ultra-Reliable Low-Latency Communications (URLLC). The proposed grant-free mechanism includes a base station, which is responsible for configuring time–frequency resources and transmission parameters for users in advance, based on the channel quality estimation of each user. The primary transmission parameters considered include Modulation and Coding Schemes (MCS) and the number of transmission attempts. These transmission parameters are selected to provide a high network capacity for up-link sporadic URLLC traffic [38]. In [39], the base station pre-allocates resources based on the packet generation interval. The study in [41] highlights the time–frequency resource allocation in the up-link for grant-based regions. While in [42], grant-free contention-based transmissions with packet repetitions are introduced to increase the reliability while respecting the latency.

Additionally, an adaptive random access protocol based on SIC is proposed in [40] to maximize system capacity. This algorithm adjusts the packet transmission probability for each time slot. The SIC decoding capability is limited to a maximum number of decodable packets. Their proposed approach integrates SIC with a tree-based splitting algorithm, where SIC operates across multiple transmissions and continues over several slots until all packets are successfully decoded. In contrast, our designed adaptive system applies SIC in each slot separately. Additionally, we adjust the required target SINR along with transmission probability. The adaptive parameter scaling is derived based on the interplay between both MAC and PHY layers, which, to the best of our knowledge, has not been previously reported in the literature. An adaptive re-transmission-based random multiple access protocol for massive machine-type communication is proposed in [43]. This protocol stabilizes the coded random access approach and estimates the number of active users. To utilize the spectrum much more efficiently along with ultra-low latency requirements the authors in [44] proposed an adaptive persistent non-orthogonal random access scheme in which each node distributively controls its transmission based on the number of active devices.

Our contribution to the state-of-the-art on SIC based multiple access is the definition of a general, yet non-trivial modeling framework to highlight the impact of transmission probability and target SINR level on system capacity with a SIC receiver. This allows a direct insight into the interplay of MAC and PHY layers, pointing at the existence of two optimal system operation regions. In this work, we also analyze the energy consumption and AoI performance in these operating regimes. Leveraging on this insight, we also contribute the assessment of stability of massive multiple access under SIC. We identify a parameter scaling strategy that leads to system stabilization, corresponding to optimized sum-rate.

3. System model

In this section, we present the system model which is tightly connected to the one introduced in [20,45].

We consider n nodes sharing a communication channel of bandwidth W. The nodes transmit to a BS over a slotted time axis. Packet size is assumed to fit into a single slot time. Packet length and slot time are denoted with L and T respectively. A transmitting node receives feedback immediately after the completion of its transmission, providing the outcome of the transmission. If unsuccessful, the node re-schedules the failed packet. We assume a non-orthogonal communication scheme. Multiple packet reception is enabled by SIC at the BS.

Multiple access is ruled according to SA or non-persistent CSMA. In the former case, a backlogged node transmits in a slot with probability p. In the latter case, a backlogged node senses the channel in a back-off slot time of size δ. If the channel is sensed to be idle, the transmission starts with probability p.

In the ensuing analysis of the sum-rate, we assume that the n nodes are saturated, i.e., they always have packets ready to send. This assumption is relaxed in the second part of the paper, where we consider non-saturated nodes and exploit the insight gained with the saturated system analysis to define an adaptive multiple access scheme.

A list of main notations used in the model is given in Table 1.

3.1. Channel model

In the following we drop the subscript i, whenever there is no ambiguity.

The path gain G is modeled as $G = G_d G_s G_f$, i.e., it is the product of a deterministic component G_d, accounting for the distance between the transmitter and the receiver, a log-normal random component G_s, accounting for shadowing due to obstacles, and a negative exponential random component G_f, accounting for multi-path Rayleigh fading.

The Two-Ray Ground (TRG) path loss model from [46] is used to account for the deterministic component G_d. Model parameters include the distance between the transmitter and the receiver, the height of the transmitter, the height of the receiver, and the carrier frequency. This model is especially apt to represent the path loss in outdoor environments, with line-of-sight reception as well as reflected electromagnetic field from the ground.

The shadowing G_s is assumed to remain the same for a given node throughout its communication activity. It is given by $G_s = 10^{\sigma_s Z/10}$, where σ_s is the shadowing standard deviation in dB and Z is a standard Gaussian random variable (zero mean, unit variance).

Table 1
Main notation used in the model.

Symbol	Definition
n	Number of nodes.
L	Packet length.
W	Channel bandwidth.
T	Packet transmission time, coincident with slot time; it is $T = L/(W\log_2(1+\gamma))$.
δ	Back-off slot time for CSMA.
β	Normalized back-off slot time, defined as $\beta = \delta/T$.
p	Back-off probability.
Γ_i	SINR of reception from node i at the BS.
γ	Target SINR.
ϵ	Maximum probability of failure of reception with no interference.
c	Defined as $c = -\log(1-\epsilon)$.
S_0	Minimum SNR to guarantee a probability of successful reception equal to $1-\epsilon$.
$P_{\text{tx},i}$	Transmission power of node i.
N_0	Noise power spectral density.
F_N	Noise figure.
P_N	Noise power level, given by $P_N = F_N N_0 W$.
$G_{d,i}$	Deterministic component of path gain of node i.
$G_{s,i}$	Shadowing component of path gain of node i.
σ_s	log-Shadowing standard deviation.
$G_{f,i}$	Rayleigh fading component of path gain of node i.
G_i	Path gain of node i, given by $G_i = G_{d,i}G_{s,i}G_{f,i}$.
S_i	SNR of reception from node i at the BS. It is $S_i = G_i P_{\text{tx},i}/P_N$.
$m_k(\gamma)$	Mean number of successfully decoded packets, when k nodes transmit.
$M_n(p,\gamma)$	Mean number of successfully decoded packets, when n nodes are backlogged.
$U_n(p,\gamma)$	Sum-rate in case of n nodes using probability of transmission p and SINR target γ.
$P_s(i)$	Probability that node's i transmission is successful.
$E(i)$	Mean energy consumed by node i per delivered packet.
$A(i)$	Mean age of information of node i at the BS.
λ	Mean message generation rate of all nodes, in case of unsaturated model.

The fading G_f depends on the variability of the propagation scenario. It is sampled from a negative exponential probability distribution with unit mean, independently packet by packet. Hence, it is $\mathcal{P}(G_f > x) = e^{-x},\ x \geq 0$.

The background thermal noise power level, P_N, is given by $P_N = F_N N_0 W$, where F_N is the noise figure and $N_0 = -174$ dBm/Hz is the thermal noise power spectral density.

3.2. Receiver model

The SINR of node i, denoted with Γ_i can be written as follows:

$$\Gamma_i = \frac{G_{d,i}G_{s,i}G_{f,i}P_{\text{tx},i}}{P_N + \sum_{j\neq i} G_{d,j}G_{s,j}G_{f,j}P_{\text{tx},j}} \tag{1}$$

Decoding of a packet transmitted by node i is deemed to be successful if $\Gamma_I \geq \gamma$, where γ is the SINR threshold, depending on the target spectral efficiency of the communication link. Assuming that additive background noise, as well as interference, can be modeled as Gaussian processes, we have an AWGN channel, and the achieved spectral efficiency is $\log_2(1+\gamma)$ for an SINR level of γ. Given that packet size is L and channel bandwidth is W, the slot size is then given by:

$$T = \frac{L}{W\log_2(1+\gamma)} \tag{2}$$

3.3. Multi-packet reception model and SIC

SIC is based on an information-theoretic framework [20]. Perfect interference cancellation is assumed with SIC, unless otherwise explicitly stated. The analysis for SIC decoding follows the similar approach used in [47,48].

Let us assume that k packets are received simultaneously and let S_j, $j = 1,\ldots,k$ be their respective Signal to Noise Ratio (SNR) levels. Assume they are ordered in descending order, i.e., $S_1 \geq S_2 \cdots \geq S_k$ (ties are broken at random). SIC works as follows. Provided decoding of packets $1,\ldots,h-1$ be successful, packet h is decoded successfully if and only if its SINR, accounting only for *residual* interference after cancellation, exceeds the threshold γ:

$$\frac{S_h}{1+\sum_{r=h+1}^{k} S_r} \geq \gamma \tag{3}$$

For comparison purposes, we consider a baseline receiver that can only exploit the capture effect, i.e., it can decode packet h successfully only if its SINR, accounting for interference from *all* concurrent transmissions, exceeds the threshold γ:

$$\frac{S_h}{1+\sum_{r=1,r\neq h}^{k} S_r} \geq \gamma \tag{4}$$

3.4. Power control

Nodes are scattered uniformly at random within a maximum distance R from the BS. Power dynamic range is limited to the interval $[P_{\text{tx,min}}, P_{\text{tx,max}}]$. We have used two different settings of power control, to compare how different settings affect sum-rate. The considered settings are as follows:

- *Scheme 1*: Equal Average Received Power (EARP). Each node aims at achieving an average received power level $P_{rx} = P_0$, same for all nodes. Equivalently, the SNR level targeted by each node is $S_0 = P_0/P_N$. This target is pursued under the constraint of a finite power dynamic range. The node has to estimate its deterministic and shadowing path gain components, e.g., through periodic pilot tones transmitted by the BS. Then, the node sets its transmission power level to compensate for those two components. Let $\hat{G}_i$ be the estimated average path gain of node i (deterministic plus shadowing components of the path gain). Then,
$$P_{\text{tx},i} = \max\left\{ P_{\text{tx,min}} \,,\, \min\left\{ P_{\text{tx,max}} \,,\, S_0 \frac{P_N}{\hat{G}_i} \right\} \right\} \tag{5}$$
The value of S_0 is chosen as follows. The received SNR for a given packet, undergoing fast fading gain G_f and in case of no interference (single transmitter), is $\Gamma = S_0 G_f$. Packet decoding is successful, if $\Gamma > \gamma$, i.e., if $G_f > \gamma/S_0$. Since G_f is a negative exponential random variable with mean 1, the probability of successful decoding in case of a single transmitter is $e^{-\gamma/S_0}$. The level S_0 is set so that this probability is at least $1-\epsilon$, i.e., $S_0 = -\gamma/\log(1-\epsilon)$.
- *Scheme 2*: Maximum transmission Power (MaxP). Each node just uses the maximum transmission power level P_{tx}, i.e., $P_{\text{tx},i} = P_{\text{tx,max}}$, $\forall i$. Every node can use this power level regardless of its position and channel conditions.

4. Model analysis

In this section the main considered performance metrics are defined and expressions for evaluating them are derived.

4.1. Probability of success

The probability of success for node i is the probability that a packet of nodes i is successfully decoded, given that node i transmits.

Let $m_k(\gamma)$ denote the mean number of successfully decoded packets in a slot with required SINR equal to γ, when k nodes transmit in that slot. Let also $s_{j,k-1}(\gamma)$ denote the conditional probability that node j delivers a packet successfully, given that node j transmits in a slot along with other $k-1$ nodes. Given these definitions, the probability of success of a generic node can be expressed in two alternative ways as:

$$P_s = \frac{1}{n}\sum_{j=1}^{n} s_{j,k-1}(\gamma) = \frac{m_k(\gamma)}{k} \tag{6}$$

It follows that:

$$m_k(\gamma) = \frac{k}{n}\left[s_{k-1}(1) + \cdots + s_{k-1}(n) \right] \tag{7}$$

for $k = 1, \ldots, n$.

The success probability of node j, given that it transmits, is obtained by weighting the conditional probability $s_h(i)$ with the probability of the event that h nodes other than node i transmits in the same slot. Hence,

$$P_s(i) = \sum_{h=0}^{n-1} s_{j,h}(\gamma)\binom{n-1}{h} p^h (1-p)^{n-1-h} \tag{8}$$

4.2. Sum-rate analysis

The overall sum-rate, U is defined as the average delivered data bit per unit of time and bandwidth. By standard argument [20], it is shown that the overall sum-rate U in case of SA is given by:

$$U = U_n(p,\gamma) = \log_2(1+\gamma)\sum_{k=1}^{n} m_k(\gamma)\binom{n}{k} p^k (1-p)^{n-k} \tag{9}$$

In case of CSMA the overall sum-rate is expressed as follows:

$$U = U_n(p,\gamma) = \log_2(1+\gamma)\,\frac{\sum_{k=1}^{n} m_k(\gamma)\binom{n}{k} p^k (1-p)^{n-k}}{\beta + 1 - (1-p)^n} \tag{10}$$

where $\beta = \delta/T$ is the normalized back-off time slot duration. Note that we assume δ is a constant, that does not scale with γ. As a consequence, β varies with γ, since T varies with γ.

In the following, we set the transmission probability p to the value that maximizes the sum-rate for each value of γ. The optimal value of the transmission probability p is denoted with $p^*(\gamma)$, to emphasize that it depends on γ. Its numerical values depends also on the adopted medium access protocol, whether SA or CSMA.

4.3. Energy

We define $E(i)$ to be the average energy consumed by node i per delivered packet, i.e., the mean of the overall amount of energy spent by node i divided by the mean number of successfully decoded packets from node i.

The energy consumed by a node i depends on its state in each time slot, as explained below:

1. *Doze state*: node i is not backlogged, hence a negligible power is consumed.
2. *Active state*: node i is backlogged, so it requires a non-null power supply, P_{ac}, for powering up processing and transceiver circuits. P_{ac} is referred as activation power.
3. *Transmit state*: node i is backlogged and transmitting as well, hence power consumed is $P_{\text{ac}} + P_{\text{tx}}(i)$.

We address first SA. The mean energy consumed by node i in a slot is given by $(P_{\text{ac}} + pP_{\text{tx}}(i))T$, since we assume saturated nodes (i.e., nodes never visit the doze state). The mean number of packets delivered by node i in a slot is $pP_s(i)$. The mean required energy per delivered packet of node i is therefore given by:

$$E(i) = \frac{(P_{\text{ac}} + pP_{\text{tx}}(i))T}{pP_s(i)} = \frac{L}{W\log_2(1+\gamma)}\left(\frac{P_{\text{ac}}}{pP_s(i)} + \frac{P_{\text{tx}}(i)}{P_s(i)}\right) \tag{11}$$

As for CSMA, we evaluate mean consumed energy and mean number of carried bits in a virtual slot time, i.e., the time elapsing between two consecutive idle back-off slots. A virtual slot time lasts δ, if no node transmits, or $\delta + T$, if at least one node transmits. In the latter case, all nodes do sensing for a time δ, then some of them transmits for a time T and the remaining ones listen to the channel over time T.

Let us focus on a given node i. The mean energy consumed in a virtual slot by node i is:

$$\begin{aligned} E_{VS}(i) \;=\; & (1-p)\left(P_{\text{ac}}\delta(1-p)^{n-1} + P_{\text{ac}}(\delta+T)[1-(1-p)^{n-1}]\right) \\ & + p\left(P_{\text{ac}}\delta + [P_{\text{ac}} + P_{\text{tx}}(i)]T\right) \end{aligned} \tag{12}$$

The mean number of packets sent by node i and successfully delivered in a virtual time slot is $pP_s(i)$, where $P_s(i)$ is the success probability of node i. So the mean energy consumed by node i can be found as follows:

$$\begin{aligned} E(i) &= \frac{E_{VS}(i)}{pP_s(i)} = \frac{P_{\text{ac}}\delta + P_{\text{ac}}T[1-(1-p)^n] + pP_{\text{tx}}(i)T}{pP_s(i)} \\ &= \frac{L}{W\log_2(1+\gamma)}\left(\frac{P_{\text{ac}}}{pP_s(i)}\left[\beta + 1 - (1-p)^n\right] + \frac{P_{\text{tx}}(i)}{P_s(i)}\right) \end{aligned}$$

Note that the success probability $P_s(i)$ and the optimized probability of transmission $p = p^*(\gamma)$ may take different values for CSMA and SA.

We define a global metric E, as the average energy per successfully delivered packet. It is given by:

$$E = \sum_{i=1}^{n} \frac{P_s(i)}{nP_s} E(i) \tag{13}$$

4.4. Age of information

When messages sent by nodes to the BS are updates or state reports collected from nodes, the freshness of state data collected from nodes is the relevant metric. AoI is meant to provide such a metric [49]. Let us consider the state reported by node i to the BS. Let $u_i(t) \le t$ be the time of the last successful delivery of a report from node i. Then the AoI of node i is $A_i(t) = t - u_i(t)$. The mean AoI is denoted with $A(i) = \mathrm{E}[A_i(t)]$. Let $Y(i)$ be the time elapsing between the delivery of two consecutive successful packets of node i. The general expression of the mean AoI is given by:

$$A(i) = \frac{\mathrm{E}[Y(i)^2]}{2\mathrm{E}[Y(i)]} \tag{14}$$

In case of SA, it is recognized that $Y(i)/T$ is a Geometric random variable with ratio equal to $pP_s(i)$. Then, it is $\mathrm{E}[Y(i)] = T/(pP_s(i))$ and $\mathrm{E}[Y(i)^2] = T^2(2 - pP_s(i))/(pP_s(i))^2$. Therefore, the mean age of information for node i is given by[1]:

$$A(i) = T\left(\frac{1}{pP_s(i)} - \frac{1}{2}\right) = \frac{L}{W\log_2(1+\gamma)}\left(\frac{1}{pP_s(i)} - \frac{1}{2}\right) \tag{15}$$

The derivation of $A(i)$ in case of CSMA starts from the same formal expression in Eq. (14), however it is rather lengthy. We refer the reader to [45, § 4.2.3].

[1] The mean AoI for a slotted random access with probability of success P_s per slot is sometimes given as $T(1/(pP_s) + 1/2)$, i.e., it differs from the expression given here by one slot. This is due to the choice of adding the duration of the slot where the considered message has been generated.

Table 2
Parameter values used in simulations.

Parameter	Value	Parameter	Value
$P_{\text{tx,min}}$	−20 dBm	$P_{\text{tx,max}}$	20 dBm
h_{tx}	2 m	h_{rx}	8 m
F_N	5 dB	W	1 MHz
σ_s	8 dB	L	2000 bits
δ	100 μs		

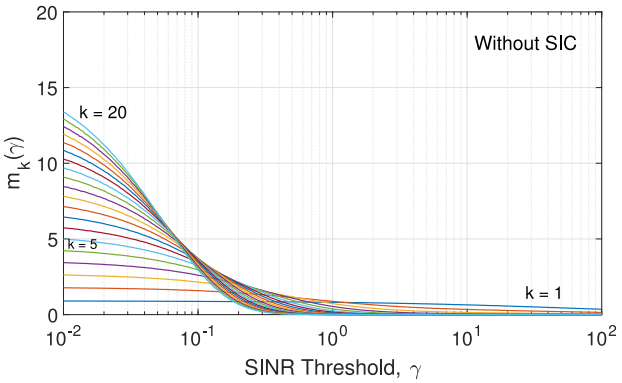

Fig. 1. Mean number of correctly decoded packets conditional on k nodes transmitting, m_k, as a function of SINR threshold γ, in case of capture effect only.

5. Performance evaluation

Performance evaluation is based on the analytical expressions given in Section 4. The only quantities that need to be derived through simulations are the mean number of correctly decoded packets per slot given in Eq. (7) and individual node probability of success given in Eq. (8). Simulations are based on an ad-hoc script in MATLAB, that implements all features of the considered networking scenario (physical layer model and MAC protocols). Given a scenario with n nodes positioned around the BS, a scenario is generated by assigning locations and shadowing gains to the n nodes. Assigned features are held fixed throughout the scenario analysis. Averaging over scenarios yields global performance metrics that can be seen as characterizing the typical node of a network made up of n nodes. All considered performance metrics are derived according to this procedure, unless otherwise explicitly stated.

Results are plotted as a function of the target SINR level γ. We consider a quite stretched range of γ values mainly to highlight the existence of different operational regimes of the system. Numerical values of the main system parameter are listed in Table 2.

5.1. Sum-rate

In this subsection, we focus on sum-rate. We recap a few results from [20], with the path loss model introduced in Section 3.2. Then, we analyze the impact of the number of nodes, the power control schemes and imperfect interference cancellation on sum-rate. Unless stated otherwise, the results presented in this subsection are specific to *EARP* power control scheme introduced in Section 3.4.

The mean number of correctly decoded packets in one transmission time slot, $m_k(\gamma)$, conditional on k nodes transmitting, is shown in Fig. 1 as a function of γ, in case of capture effect only (no SIC). Fig. 2 shows m_k in case of SIC. Both these figures are shown for several values of k, ranging from 1 to 20.

In both cases, m_k is monotonously decreasing with γ, which is quite intuitive, since higher values of γ are more challenging for the receiver. Another common feature of m_k plots is that $m_1 > m_k$, $\forall k > 1$, for sufficiently large values of γ, both with and without SIC. This shows that it is best to avoid concurrent transmissions in high spectral efficiency regime (large γ). On the contrary, for small γ values, the higher k, the bigger the number of correctly decoded packets. In fact, for very low γ values, interference cancellation is quite effective and even capture works fine for many packets. The main difference between the results with SIC and without SIC lies with the behavior of curves for intermediate values of γ. The transition in case of SIC is much sharper than in case of capture only, denoting a sort of threshold effect.

Fig. 3 shows the sum-rate as a function of γ. The solid and dashed blue lines represent SA with and without SIC, respectively. The dotted and dash-dotted red lines represent CSMA with and without SIC, respectively. Two peaks appear in Fig. 3, one in the low γ range and another one in the high γ range. As for capture-only performance, the highest sum-rate is achieved for relatively high values of γ, while low spectral efficiency operation leads to very low sum-rate values. Moreover, CSMA turns out to offer superior sum-rate performance with respect to SA, which is a well-known classic result. The peak of sum-rate shows that essentially the same performance is achieved with and without SIC. In other words, when working in the high spectral efficiency regime (high values of γ), SIC provides little gain to random access protocols in terms of throughput. Note that the high spectral efficiency regime is the typical choice of cellular system as well as WiFi.

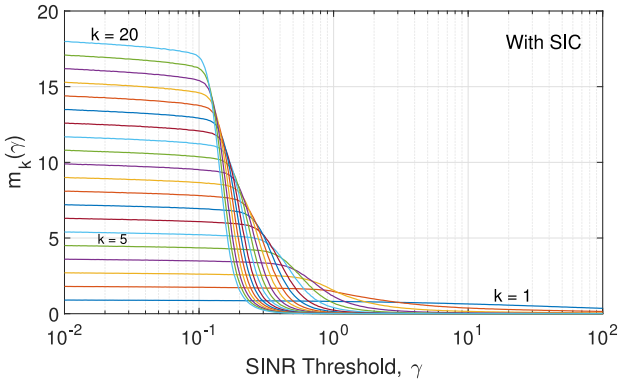

Fig. 2. Mean number of correctly decoded packets conditional on k nodes transmitting, m_k, as a function of SINR threshold γ, in case of SIC at the receiver.

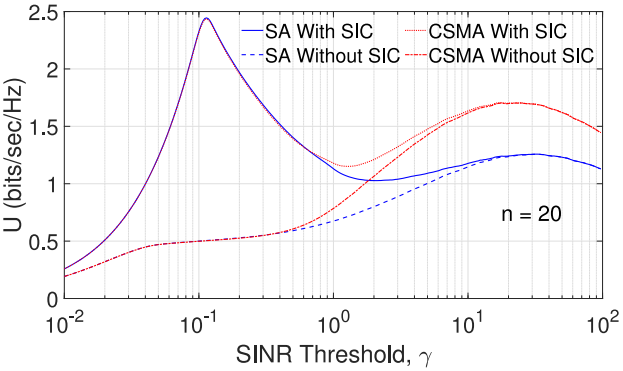

Fig. 3. Sum-Rate U as a function of SINR threshold γ for the optimized value of the transmission probability p. (For interpretation of the references to color in this figure legend, the reader is referred to the web version of this article.)

In case of SIC, a second peak of sum-rate appears for lower values of γ, i.e., when the system is operated in a low spectral efficiency regime. The physical layer (SIC) is mainly responsible for improving the system performance while the role of MAC layer is negligible, in low spectral efficiency regime, because all the nodes are allowed to transmit simultaneously, i.e., the optimal transmission probability is 1. This is the region of choice of spread-spectrum systems or some sensor network technology, e.g., LoRaWAN. The same optimized performance is achieved by SA and CSMA at this left peak of sum-rate, which is consistent with the fact that the MAC protocol plays essentially no role. When only capture effect is exploited (no SIC), the achieved sum-rate is quite low, definitely worse than what can be achieved at high γ values. If SIC is in place, a strong improvement of sum-rate is obtained, even better than what is achieved for large γ. For large values of γ, the MAC layer is the bottleneck, since collisions are mainly responsible for the performance degradation.

5.1.1. Impact of the number of nodes

Results shown up to here refer to a fixed number of nodes, $n = 20$. Now we highlight the sensitivity of sum-rate in the two identified regimes, with respect to the number of contending nodes n. The sum-rate with and without SIC for several values of the number of nodes n is shown in Figs. 4 and 5 in case of SA and CSMA respectively. These plots offer valuable insights into the system's behavior as the number of nodes varies. When nodes are few, there is no point in using low spectral efficiency, i.e., a low value of γ. As the number of contending nodes n increases, using high values of γ and limiting the number of concurrent transmissions by reducing p is the best strategy without SIC.

On the contrary, with SIC, the sum-rate peak in low spectral efficiency regime moves to the left, while the sum-rate peak in the high spectral efficiency regime fades away, due to collisions. The SIC-enabled physical layer allows most or all nodes to transmit, but at the same time it forces nodes to pick low γ values to get decoded successfully. Hence, the optimal γ providing the sum-rate peak decreases as n grows. In this low threshold regime, there is no need for MAC regulation. Grant-free transmissions are enabled by the multi-packet reception capability of SIC.

5.1.2. Impact of power control

The power control schemes defined in Section 3.4 are compared in this section in terms of sum-rate for SA and CSMA. In Section 5.1 we have discussed the results obtained with *EARP* power control scheme, where the average received power is same for

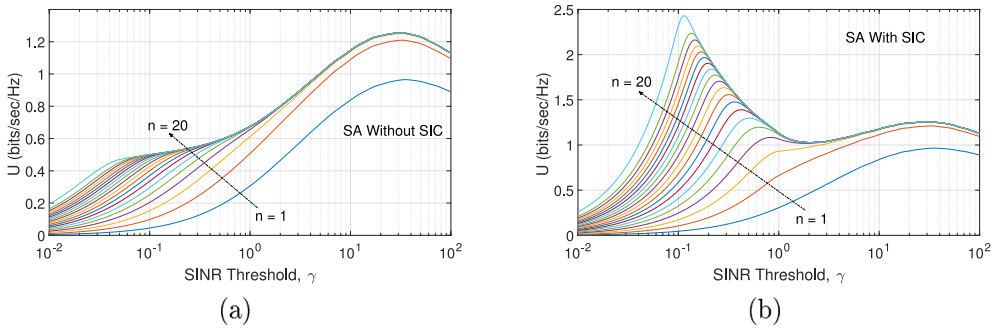

Fig. 4. Sum-Rate U as a function of SINR threshold γ for the optimized value of the transmission probability p, for several values of the number of nodes n, in case of SA. (a) Without SIC. (b) With SIC.

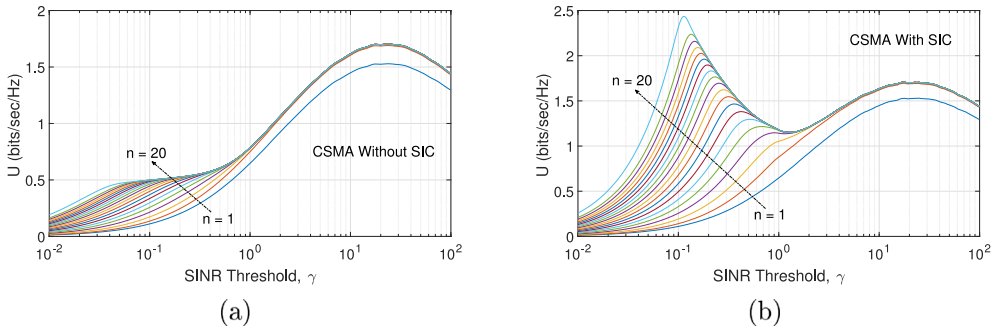

Fig. 5. Sum-Rate U as a function of SINR threshold γ for the optimized value of the transmission probability p, for several values of the number of nodes n, in case of CSMA. (a) Without SIC. (b) With SIC.

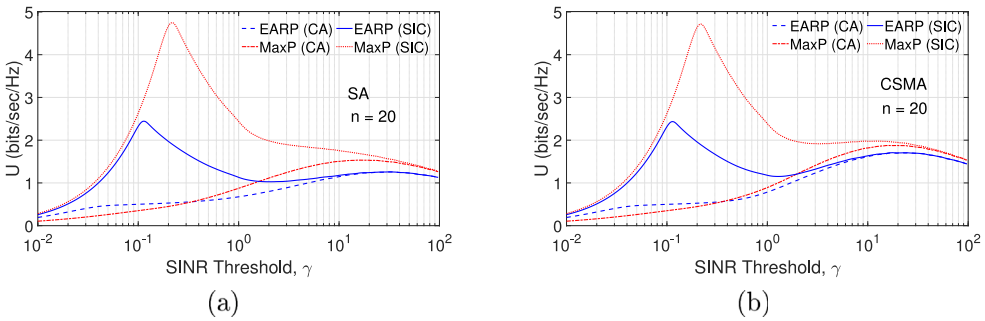

Fig. 6. Sum-rate U as a function of SINR threshold γ for the optimized value of the transmission probability p (With power control). (a) SA. (b) CSMA.

all the nodes. In this section, the blue solid and dashed lines refer to power *EARP* with and without SIC, respectively, while the red dotted and dash-dotted lines refer to power *MaxP* with and without SIC, respectively.

Fig. 6(a) plots the sum-rate for SA as a function of γ for the two power setting schemes with and without SIC. The overall sum-rate in the low threshold regime is increased significantly by using *MaxP*. This is intuitive, as we are inducing a difference in the received power levels of different nodes with respect to *EARP* and SIC is exploiting this difference to decode more packets successfully.

The sum-rate performance for CSMA, for the given two power setting schemes are shown in Fig. 6(b). There exists a slight difference w.r.t SA results, shown in Fig. 6(a). CSMA results offer some advantage over SA in high γ regime, for both power setting schemes, which is a well-known classic result. On the contrary, in case of low γ regime, either the results are similar or SA has a slight edge over CSMA for *MaxP*. Remember that the MAC layer is essentially playing no role in low γ regime, so the gain is only due to the physical layer i.e, due to SIC.

5.1.3. Impact of imperfect interference cancellation

In this subsection, we identify the impact of imperfect interference cancellation for *EARP*. Similar results can be obtained for *MaxP* in terms of the reduction of sum-rate performance achieved with perfect cancellation.

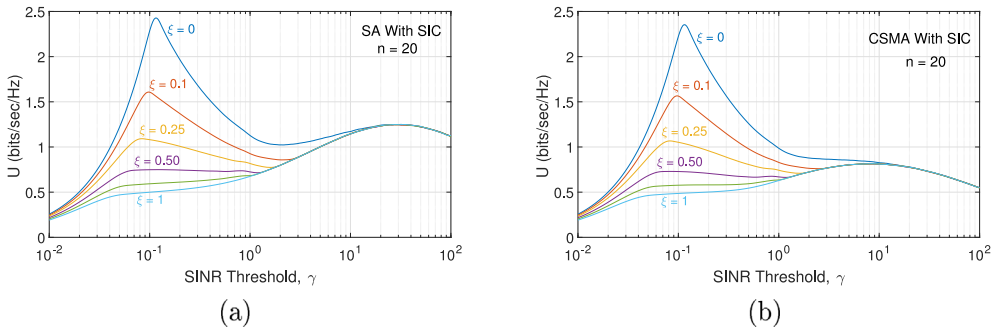

Fig. 7. Sum-Rate U in case of imperfect interference cancellation as a function of SINR threshold γ for the optimized value of the transmission probability p and for several values of the interference cancellation factor ξ. (a) SA. (b) CSMA.

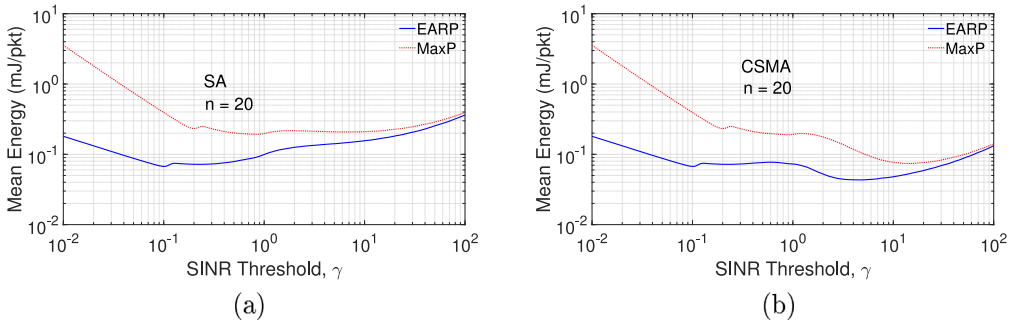

Fig. 8. Mean energy as a function of SINR threshold γ with different power setting schemes. (a) SA. (b) CSMA. (For interpretation of the references to color in this figure legend, the reader is referred to the web version of this article.)

Imperfect SIC is modeled through a single parameter, $\xi \in [0, 1]$, which is the fraction of signal power left over after cancellation. With reference to the multi-packet reception model outlined in Section 3.3, let $S_1, \ldots, S_k$ be the SNR levels of the k simultaneously transmitting nodes, sorted in descending order. The h-node's packet is decoded successfully if all previous packets from 1 to $h-1$ have been successfully decoded and additionally we have[2]

$$\frac{S_h}{1 + \xi \sum_{i=1}^{h-1} S_i + \sum_{i=h+1}^{k} S_i} \geq \gamma \tag{16}$$

for $h = 1, \ldots, k$. For $\xi = 0$ this expression reduces to the one in Eq. (3) (perfect cancellation).

Fig. 7 shows the sum-rate as a function of γ for $n = 20$ saturated nodes and for several values of the residual interference coefficient ξ, ranging between 0 (perfect cancellation) up to 1 (no cancellation at all, i.e., no SIC). It shows that even 10%–25% of residual interference causes a strong degradation of the sum-rate performance. These results hint at the requirement of a highly accurate interference cancellation to reap a substantial sum-rate gain in low spectral efficiency regime with respect to high spectral efficiency regime.

5.2. Energy per delivered packet and AoI

In this section, we discuss mean energy consumed per delivered packet and mean AoI for both SA and CSMA. Separate figures are shown for SA and CSMA, with blue curves referring to *EARP*, and red curves to *MaxP* power settings.

The mean energy averaged across all nodes is plotted in Fig. 8, for both SA and CSMA with the *EARP* and *MaxP*.

From the leftmost part of the plots, it is apparent that mean energy required to deliver one packet to the BS increases as γ decreases, notably faster for *MaxP* for both SA and CSMA. This is due to a number of reasons, primarily the increase of slot size as γ decreases. As we move towards higher values of γ, reception becomes more challenging, and success probability starts falling off to quite low values at some point. To confirm this analysis, the success probability is plotted in Fig. 9, for both power setting schemes in case of SA and CSMA.

On the other hand, transmission becomes more spectrally efficient, and much less time is spent to transmit one packet (the slot time size becomes smaller). The balance of these two contrasting forces drives energy consumption to grow eventually as γ

[2] Note that received signal power sorting is irrelevant in case $\xi = 1$, i.e., there is no SIC.

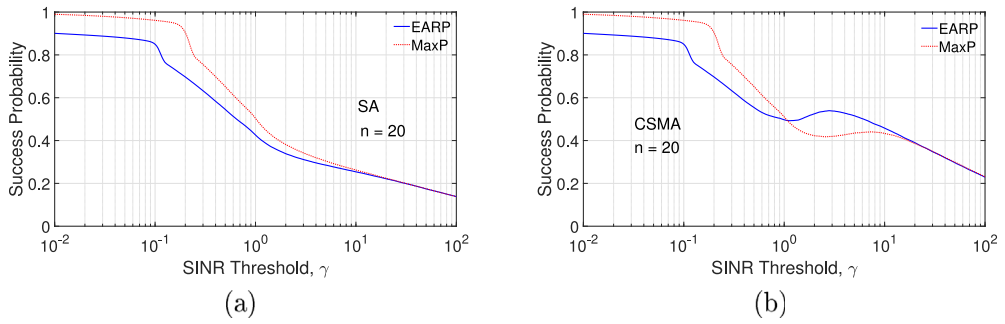

Fig. 9. Probability of success P_s, as a function of SINR threshold γ with different power setting schemes. (a) SA. (b) CSMA.

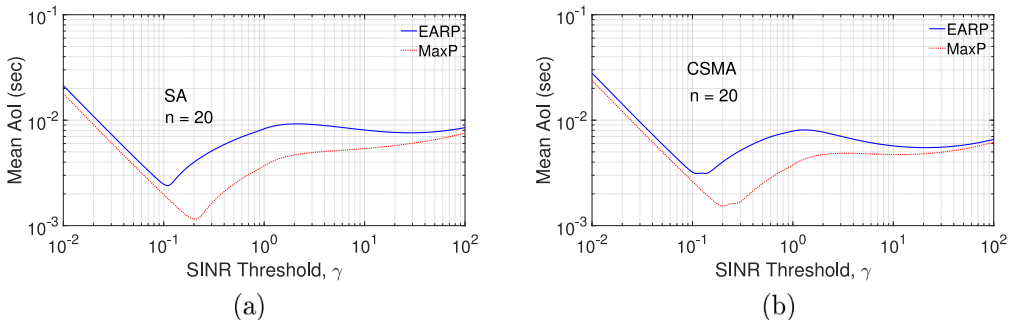

Fig. 10. Mean AoI as a function of SINR threshold γ with different power setting schemes. (a) SA. (b) CSMA.

increases, as visible from the curve of *EARP*. *EARP* turns out to be much more energy efficient than *MaxP*. This result stems mainly from the fact that transmission power in *EARP* is tailored for each node so that the average receive power is the minimum required to guarantee a given level of success probability in case of no interference. In other words, *EARP* is enforcing a parsimonious power control, however giving up to power diversity that is helpful to SIC. On the contrary, *MaxP* try to differentiate the average receive power levels of nodes, to improve SIC.

In case of CSMA, there exists a transition region in which the mean energy drops down and then it grows slowly. This drop down is due to the non-trivial behavior of success probability due to the decreasing value of the optimal transmission probability as γ grows. Hence, the average number of concurring transmissions decreases, boosting the value of success probability. As γ grows further, success probability definitely falls down, since the effect of the limited maximum transmission power level prevails. Also at some point the mean energy turns out to be same for both power setting schemes, increasing γ is forcing the nodes to adjust high transmission power level, due to power limitation we see a convergence of both power setting schemes.

The mean AoI averaged across all nodes is plotted in Fig. 10 in case of SA and CSMA with the two considered power schemes.

The mean AoI with *EARP* is slightly higher than with *MaxP*. This difference is less in low γ regime as compared to transition and high γ regime. In low γ regime, the mean AoI increases as γ becomes smaller, essentially due to growing slot sizes. In case of high γ regime, the success probability decreases due to high requirement at the physical layer receiver, that will be not met eventually, due to limited power dynamics. As a result, the mean AoI grows for both power setting schemes in the high γ regime, even though a back-off probability less than 1 induces smaller slot sizes. Compared to CSMA, mean AoI for both power setting schemes is lower in case of SA.

Comparing mean energy per delivered packet and mean AoI for SA and CSMA and for the two considered power setting schemes, it is apparent that EARP offers better performance in terms of consumed energy at the price of a worse freshness of collected data. No big difference is brought by changing the multiple access protocol. Finally, the best choice of the target SINR level γ that minimizes AoI is somewhat offset with respect to the choice of γ that minimizes consumed energy, showing that there exists a trade-off between these two metrics.

6. Non-saturated model

In this section, leveraging on insight gained in the previous analysis, we address the definition of an adaptive algorithm to stabilize the SIC-based multiple access system in a non-saturated environment. Adaptation consists of varying the probability of transmission p and target SINR γ as a function of the number of nodes that are backlogged at the beginning of each time slot, so as to guarantee that the system is stable, i.e., the mean number of backlogged nodes has a finite mean. Practical stabilization algorithms can be devised by building estimators of the number of backlogged nodes. As a matter of example, the number of contending nodes

can be estimated by the classic pseudo-Bayesian algorithm proposed in [50] for general non-persistent CSMA algorithms, or by the Kalman filter approach defined in [51] for the basic IEEE 802.11 MAC protocol and in [52] for the IEEE 802.11e MAC protocol with priority handling. We do not dwell on investigating the implementation of such estimators in the present case of SIC-assisted multiple access, rather we are primarily interested in assessing stability conditions under an idealized adaptive scheme, where the number of backlogged nodes at the beginning of the slot is assumed to be exactly known.

6.1. Model description and assumptions

Time is slotted with variable size slots. Let $Q(t)$ denote the number of nodes backlogged at the beginning of slot t. Both the target SINR γ and the transmission probability p are functions of $Q(t)$. If $Q(t) = k$, then $\gamma = \gamma_k$ and $p = p_k$, where γ_k and p_k for $k \geq 1$ are assigned sequences. The sequence $\{\gamma_k\}_{k\geq 1}$ must be bounded to make power control feasible. We let $\gamma_{\max} = \max_{k\geq 1} \gamma_k$.

Since a node adjusts its transmitting power and coding scheme to conform to the required SINR, given $Q(t) = k$, the slot size is:

$$T_k = \frac{L}{W \log_2 (1 + \gamma_k)} \tag{17}$$

If no node is backlogged in a slot, the slot size reduces to a fixed time T_0.

Decoding of concurrently transmitted packets occurs using SIC, as described in Section 3.3. The condition for successful decoding are as described with reference to Eq. (3), simply replacing γ with $\gamma_{Q(t)}$ and k with $K(t)$ where $K(t)$ is the outcome of a binomial random variable with parameters $Q(t)$ and $p_{Q(t)}$.

We assume an infinite population of nodes. Nodes become backlogged upon message generation. The generation of new messages by the node population follows a Poisson process with mean arrival rate Λ. A node handles one message at a time. When it is backlogged, no new arrivals are considered. A backlogged node transmits in slot t with probability $p_{Q(t)}$. A node will know the outcome of its transmission attempt by the end of the slot. In case of failure, the node will re-schedule the message and make new transmission attempts, until its message is delivered to the BS successfully. Upon successful delivery, the node returns to the pool of idle nodes.

As for the physical channel, we assume the same model as in Section 3.1, except that shadowing is neglected.[3] Hence the power level received at the BS from a node at distance r is $P_{\text{rx}} = G_{\text{d}}(r) G_{\text{f}} P_{\text{tx}}$, where $G_{\text{d}}(r)$ is computed according to the TRG path loss model from [46] and G_{f} is a negative exponential random variable with mean 1, accounting for Rayleigh fading.

In this section we restrict our attention to *EARP*. We consider the worst case power budget for nodes within a distance R of the BS. The maximum allowable distance is evaluated by finding the largest R such that $G_{\text{d}}(R) P_{\text{tx,max}} / P_N \geq \gamma_{\max}/c$. Under this condition, i.e., for any node at distance $r \leq R$ of the BS, it is always possible to set P_{tx} in slot t so that $G_{\text{d}}(r) P_{\text{tx}} / P_N = \gamma_{Q(t)}/c$.

6.2. Stability of the multiple access channel

The time evolution of the number of backlogged nodes is described by the following one-step equation:

$$Q(t+1) = Q(t) + A(t) - D(t) \tag{18}$$

where,

- $Q(t)$ is the number of nodes backlogged at the beginning of slot t.
- $A(t)$ is the number of nodes that become backlogged in slot t.
- $D(t)$ is the number of packets that are successfully decoded by the BS in slot t. The nodes whose packet is acknowledged go back to idle state.

It is apparent that $Q(t)$ is an irreducible, aperiodic DTMC on the state space of non negative integers. To assess under which condition it is positive recurrent, we resort to Foster–Lyapunov theorem [53]. The mean conditional drift of the DTMC is defined as follows for $n \geq 1$:

$$\Delta_n = \mathrm{E}[Q(t+1) - Q(t) \mid Q(t) = n] = \mathrm{E}[A(t) \mid Q(t) = n] - \mathrm{E}[D(t) \mid Q(t) = n] \tag{19}$$

To apply that theorem to our case, we only need to check that the $\limsup_{n\to\infty} \Delta_n < 0$ (see Appendix B for a proof of this statement).

Given that the arrival of new nodes follows a Poisson process, the average number of arrivals in a slot, conditional on $Q(t) = n$, is:

$$\mathrm{E}[A(t) \mid Q(t) = n] = \Lambda T_n = \frac{\Lambda L}{W \log_2(1 + \gamma_n)} \tag{20}$$

The mean number of departures, conditional on $Q(t) = n$, is:

$$\mathrm{E}[D(t) \mid Q(t) = n] = \sum_{k=1}^{n} m_k(\gamma_n) \binom{n}{k} (p_n)^k (1 - p_n)^{n-k} \tag{21}$$

[3] Shadowing turns the deterministic worst case analysis of received power into a probabilistic bound. While requiring a more cumbersome notation, shadowing does not add anything to the discussion of the stability in the rest of this section.

where $m_k(\gamma)$ is the mean number of packets successfully decoded, when k nodes transmit and the target SINR is γ.

Using Eqs. (9), (20) and (21), the conditional drift can be written as follows for $n \geq 1$:

$$\Delta_n = \frac{1}{\log_2(1+\gamma_n)} \left[\frac{\Lambda L}{W} - U_n(p_n, \gamma_n) \right] \tag{22}$$

To prove the stability of $Q(t)$, based on Foster–Lyapunov theorem, it is enough to verify that $\limsup_{n\to\infty} \Delta_n < 0$. For that purpose we consider the following scaling: $\gamma_n = 1/(bn)$ and $p_n = 1$. The considered scaling corresponds to a grant-free multiple access, where all backlogged nodes are allowed to transmit in the same slot, targeting at low rate, specifically, with a target SINR inversely proportional to the number of backlogged nodes. The scaling is set so as to match the sum-rate maximum in the low spectral efficiency region, highlighted in the analysis of Section 5 (see Figs. 4 and 5).

With the chosen scaling, it is $U_n(p_n, \gamma_n) = \log_2(1 + 1/(bn)) \cdot m_n(1/(bn))$. In Appendix A it is proved that, under this scaling and under the assumptions holding for the considered multiple access channel model, it is:

$$m_n(1/(bn)) \sim \zeta(b)\, n\,, \qquad n \to \infty\,, \tag{23}$$

where $\zeta = \zeta(b)$ is defined as follows:

$$\zeta = \sup \left\{ x \in (0,1] : f_b(z) \geq c, \forall z \in (0,x) \right\} \tag{24}$$

with

$$f_b(z) = -\left(1 + \frac{z}{b}\right) \log z - \frac{1-z}{b}\,, \qquad z \in (0,1] \tag{25}$$

From its definition, it is apparent that ζ is the smallest positive root of $f_b(x) = c$ for $x \in (0,1)$. Roots of this equation in $(0,1)$ exist surely for $c > 0$, since $f_b(x)$ is continuous for $x > 0$, it tends to $+\infty$ as $x \to 0^+$ and it tends to 0 as $x \to 1$.

Leveraging on this asymptotic result, it is found that:

$$\lim_{n\to\infty} U_n\left(1, \frac{1}{bn}\right) = \lim_{n\to\infty} \log_2\left(1 + \frac{1}{bn}\right) m_n\left(\frac{1}{bn}\right) = \frac{\zeta(b)}{b \log 2} \tag{26}$$

This limit holds for any positive b. Hence, we have for the drift:

$$\Delta_n \sim n\, b\, \log 2 \left[\frac{\Lambda L}{W} - \frac{\zeta(b)}{b \log 2} \right] \qquad n \to \infty \tag{27}$$

The drift is definitely negative as n grows, provided that:

$$\Lambda < \frac{W}{L} \frac{\zeta(b)}{b \log 2} \tag{28}$$

As for b, we set it to the value that maximizes the right-hand side of Eq. (28). Since, by its definition, ζ belongs to the interval $(0,1)$ and it behaves as $(1-\epsilon)e^{-1/b}$ as $b \to 0^+$, it follows that the maximum of $\zeta(b)/b$ exists and it is attained for some $b^* > 0$.

6.3. Numerical results

Leveraging on the result of Section 6.2, we set the adaptive parameters as follows, given a threshold $n_{\max}$:

$$\gamma_n = \begin{cases} \gamma_n^* & 1 \leq n \leq n_{\max}, \\ \frac{1}{b^* n} & n > n_{\max}. \end{cases} \qquad p_n = \begin{cases} p_n^* & 1 \leq n \leq n_{\max}, \\ 1 & n > n_{\max}. \end{cases} \tag{29}$$

where γ_n^* and p_n^* denote the values of γ and p that maximize the sum rate $U_n(\cdot,\cdot)$, to be found numerically for $1 \leq n \leq n_{\max}$, and $b^* = \text{argmax}_{b>0} \frac{\zeta(b)}{b \log 2}$.

Simulations of the adaptive algorithm have been run with the following parameter values: $L = 2000$ bit, $W = 1$ MHz, $T_0 = 1$ ms, $\epsilon = 0.1$, $\gamma_{\max} = 100$, $n_{\max} = 50$. It is found that $b^* \approx 0.39$ and $\zeta(b^*) \approx 0.81$. Based on all the given values $U_{asy} = 2.99$. We set $\Lambda = \rho \Lambda^*$, where $\Lambda^* = \frac{W}{L} \frac{\zeta(b^*)}{b^* \log 2} = \frac{W U_{asy}}{L}$, with $\rho = 0.9$.

The optimal transmission probability p_n^* and SINR target γ_n^* as a function of n are shown in Fig. 11. It is noted that optimal parameter values for small n (up to $n = 3$) can be approximated as $p_n^* \approx 1/n$ and $\gamma_n^* = \gamma_{\max}$, whereas for larger n they match the trend of the adopted scaling.

The time evolution of a sample path of $Q(t)$, starting from $Q(0) = 0$, is shown in Fig. 12(a). Fig. 12(b) shows the cumulative time-averaged sum-rate $\overline{U}(t)$ as a function of time. $\overline{U}(t)$ is defined as:

$$\overline{U}(t) = \frac{1}{t} \sum_{\tau=1}^{t} U(\tau) \tag{30}$$

where $U(\tau)$ is the sum rate realized in slot τ.

It is apparent from these plots that the queue is under control (fluctuations do not diverge) and the time-averaged sum-rate tends to 90% of its asymptotic value ($0.9 \cdot 2.99 = 2.69$), which is the maximum that can be obtained, given the load $\rho = 0.9$.

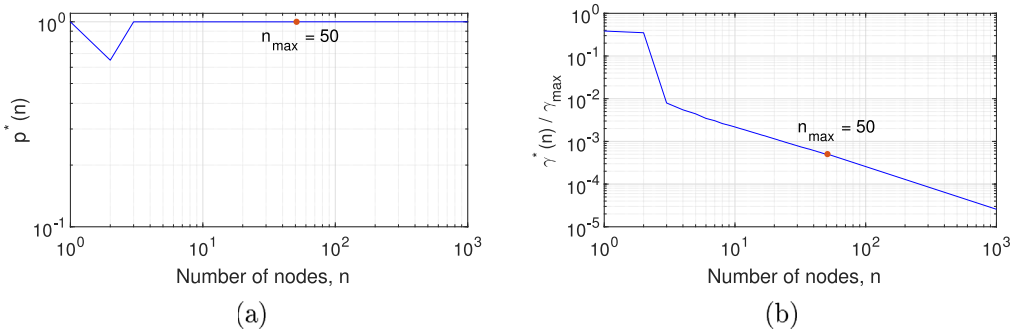

Fig. 11. Optimal value of system parameters when n nodes are backlogged. (a) Probability of transmission p_n^*. (b) Normalized target SINR $\gamma_n^*/\gamma_{\max}$.

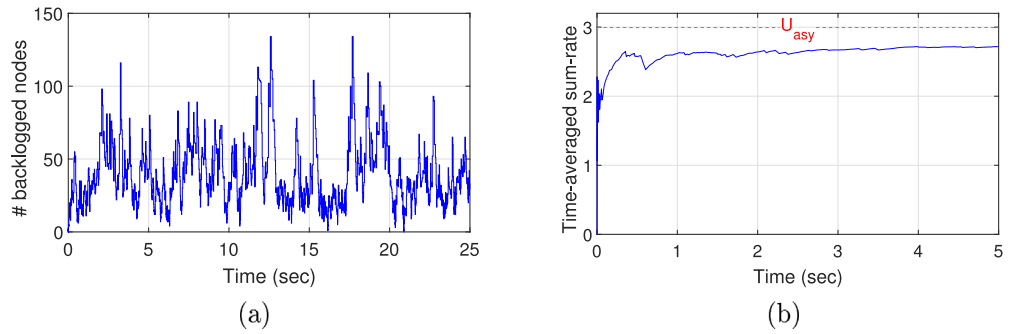

Fig. 12. Evolution of the adaptive multiple access system over time: (a) Number of backlogged nodes, $Q(t)$. (b) Time-averaged sum-rate, $\overline{U}(t)$.

7. Conclusion

We have defined a modeling framework rich enough to capture the effect of SIC in a non-orthogonal multiple access system as key system parameters are varied, namely the probability of transmission in a slot and the target SINR. The model results highlight that the system sum-rate exhibits two local maxima, one of which disappears if we remove SIC. Specifically, the system can be run in two ways.

1. A high spectral efficiency is targeted and random access algorithms are used to reduce the number of collisions that cannot be solved by SIC.
2. A low spectral efficiency communication is used, allowing multiple concurrent transmissions that are dealt with by SIC (grant-free multiple access).

The former approach yields well-known results, e.g., CSMA outperforms SA. In this regime, essentially one of the few transmissions in each time slot can be accommodated with success. Performance is dominated by the MAC algorithm and little can be added via SIC. On the opposite, in the latter case, an even higher overall sum-rate can be achieved, exploiting SIC, at least as long as interference cancellation is accurate. In this second regime, performance is determined by the physical layer while the role of MAC fades away.

The extensive performance analysis shown in this paper, including sum-rate, success probability, consumed energy, and age of information, shows that the second regime (low spectral efficiency communications) is also able to optimize all other considered performance metrics. On the contrary, the high spectral regime introduces unfairness (nodes further from the BS are penalized) and fails to provide good energy and AoI performance.

The insight gained in this analysis allows defining an adaptive parameter setting scaling to accommodate a time-varying number of backlogged nodes, guaranteeing the overall system stability.

There are many directions that this work could be carried over. We emphasize two of them: (i) providing practical algorithms for implementing SIC and characterizing the complexity of the receiver as well as the loss of achieved performance with respect to the idealized SIC considered in this paper; (ii) defining a practical adaptive algorithm that estimates the required p and γ, based on a reinforcement learning approach.

Funding

This work was partially supported by the European Union under the Italian National Recovery and Resilience Plan (NRRP) of Next Generation EU, a partnership on “Telecommunications of the Future” (B53C22004050001 - program “RESTART”).

CRediT authorship contribution statement

Asmad Bin Abdul Razzaque: Writing – review & editing, Writing – original draft, Visualization, Validation, Software, Methodology, Investigation, Formal analysis, Conceptualization. **Andrea Baiocchi:** Writing – review & editing, Writing – original draft, Visualization, Validation, Supervision, Project administration, Methodology, Investigation, Funding acquisition, Formal analysis, Conceptualization.

Declaration of competing interest

The authors declare that they have no known competing financial interests or personal relationships that could have appeared to influence the work reported in this paper.

Appendix A. Proof of asymptotic behavior of number of decoded packets in a slot

Let us assume n nodes transmit simultaneously in a time slot. We aim to prove that the mean number of successfully decoded packets $m_n(\gamma)$ scales linearly with n, if we set $\gamma = 1/(bn)$. Formally, we prove that:

$$m_n(1/(bn)) \sim \zeta(b)\, n \tag{A.1}$$

as $n \to \infty$, where $\zeta(b)$ is a suitable constant, depending on the scaling parameter b.

Under the considered propagation model, the power level received at the BS from node j is given by $Y_j\gamma/c$, where Y_j is a random variable, accounting for Rayleigh fading. We assume nodes are numbered in descending order of received power (from the strongest to the weakest received signal). Hence $Y_1 \geq Y_2 \geq \cdots \geq Y_n$ is the order statistics of a set of n i.i.d. negative exponential random variables with mean 1.

Re-arranging Eq. (3) with $S_j = Y_j\gamma/c$, it is found that the kth strongest packet is successfully decoded, if the following inequalities are met for $h = 1, \ldots, k$:

$$Y_h \geq c + \gamma \sum_{r=h+1}^{n} Y_r \tag{A.2}$$

The density function of Y_h $(h = 1, \ldots, n)$ is:

$$f_h(x) = \frac{n!}{(n-h)!(h-1)!} e^{-hx}(1-e^{-x})^{n-h}, \qquad x \geq 0. \tag{A.3}$$

It can be verified that $f_n(x) = ne^{-nx}$ and $f_h(x) = f_{h+1}(x) \star (he^{-hx})$, for $h = 1, \ldots, n-1$, where $\star$ denotes convolution. Applying this equality iteratively, it follows that $f_h(x) = (he^{-hx}) \star \ldots \star (ne^{-nx})$. Since je^{-jx} is the density function of a negative exponential random variable with mean $1/j$, the following representation holds:

$$Y_h = \sum_{j=h}^{n} \frac{X_j}{j} \tag{A.4}$$

where $X_1, X_2, \ldots, X_n$ are i.i.d. negative exponential random variables with mean 1. Substituting this representation into Eq. (A.2) and re-arranging, we get:

$$V_h = \sum_{j=h}^{n} a_{h,j} X_j \geq c \tag{A.5}$$

with

$$a_{h,j} = \frac{1+h\gamma}{j} - \gamma, \qquad j = h, \ldots, n,\ h = 1, \ldots, n. \tag{A.6}$$

Using the variables V_h, successfully decoding at least k packets out of n is equivalent to the k inequalities: $V_h \geq c$ for $h = 1, \ldots, k$. In the following, it will be shown that V_{nx} tends to a deterministic random variable with mean $f_b(x)$ (see Eq. (25)) as $n \to \infty$, for any $0 < x \leq 1$. Then, as n grows, we have $V_{nx} \geq c$ w.p. 1 for all $x < \zeta$ and $V_{nx} < c$ w.p. 1 for all $x > \zeta$, where ζ is defined in Eq. (24).

In the asymptotic regime, we set $\gamma = \gamma_n = 1/(bn)$ and $h = nx$, with $0 < x \leq 1$. The mean of $V_h|_{h=nx}$ is:

$$\mathrm{E}[V_{nx}] = \left(1 + \frac{x}{b}\right) \sum_{j=nx}^{n} \frac{1}{j} - \frac{1-x}{b} \sim -\left(1 + \frac{x}{b}\right) \log x - \frac{1-x}{b} = f_b(x) \tag{A.7}$$

where we have used the asymptotic relationship of harmonic numbers $\sum_{j=1}^{n} 1/j \sim \log n$, to derive that $\sum_{j=nx}^{n} 1/j \sim \log n - \log(nx) = -\log x$ as $n \to \infty$.

As for the variance, we have:

$$\sigma^2_{V_{nx}} = \left(1 + \frac{x}{b}\right)^2 \sum_{j=nx}^{n} \frac{1}{j^2} + \frac{1-x}{nb^2} - \frac{2}{b}\left(1 + \frac{x}{b}\right) \frac{1}{n} \sum_{j=nx}^{n} \frac{1}{j} \sim 0 \tag{A.8}$$

as $n \to \infty$, since $\sum_{j=nx}^{n} 1/j^2$ is upper bounded by the remainder of the convergent series $\sum_{j=1}^{\infty} 1/j^2$.

Let ϵ be an arbitrary positive number and let $n > N_\epsilon$, where N_ϵ is set so that $\left|\mathrm{E}[V_{nx}] - f_b(x)\right| < \epsilon$, $\forall n > N_\epsilon$. Then, using Eqs. (A.7) and (A.8), we have for any $n > N_\epsilon$:

$$\begin{aligned}\mathcal{P}\left(\left|V_{nx} - f_b(x)\right| > 2\epsilon\right) &\le \mathcal{P}\left(\left|V_{nx} - \mathrm{E}[V_{nx}]\right| + \left|\mathrm{E}[V_{nx}] - f_b(x)\right| > 2\epsilon\right) \\ &\le \mathcal{P}\left(\left|V_{nx} - \mathrm{E}[V_{nx}]\right| > \epsilon\right) \le \frac{\sigma^2_{V_{nx}}}{\epsilon^2} \end{aligned} \tag{A.9}$$

The last passage is a consequence of Chebyshev inequality. Since the variance of V_{nx} vanishes as n grows to infinity, this proves that V_{nx} tends asymptotically to the deterministic quantity $f_b(x)$ with probability 1 as $n \to \infty$, for any given $x \in (0, 1]$.

Given that we can replace V_{nx} with its mean $f_b(x)$ asymptotically, it is seen that $m_n(\gamma)|_{\gamma=1/(bn)} \sim \zeta n$ packets are decoded successfully where ζ is defined in Eq. (24), and hence ζ is the least positive root of $f_b(x) = c$. The existence of such a root is due to the following facts: (i) $c > 0$; (ii) $f_b(x)$ is continuous for $x \in (0, 1]$; (iii) $f_b(x) \to +\infty$ as $x \to 0^+$; (iv) $f_b(1) = 0$.

Appendix B. Application of Foster–Lyapunov theorem to the DTMC $Q(t)$

For ease of readers, we state Foster–Lyapunov theorem below.

Theorem 1 (*Foster–Lyapunov*). *Let $\{X_k\}_{k\ge 0}$ be an irreducible Markov chain on the state space $\mathcal{S}$. Assume there exists a function $V : \mathcal{S} \mapsto \mathbb{R}$, with $V(x) \ge 0$, $\forall x \in \mathcal{S}$, and a finite set $\mathcal{A} \subseteq \mathcal{S}$ such that $\mathrm{E}[V(X_0)] < \infty$ and the following conditions hold:*

1. $\mathrm{E}[V(X_{k+1}) - V(X_k)|X_k = x] \le -\epsilon$, *if* $x \in \mathcal{S} \setminus \mathcal{A}$
2. $\mathrm{E}[V(X_{k+1}) - V(X_k)|X_k = x] \le b$, *if* $x \in \mathcal{A}$

for a given $\epsilon > 0$ and a finite constant b. Then the Markov chain X_k is positive recurrent.

Theorem 1 is applicable to the DTMC $Q(t)$, $t \ge 0$, defined in Eq. (18) over the state space of non-negative integers: $\mathcal{S} = \{0, 1 \dots\}$. We consider the function $V(x) = x$. Letting time $t = 0$ be the beginning of a busy period, we have $Q(0) = 0$, hence $\mathrm{E}[V(Q(0))] = \mathrm{E}[Q(0)] = 0$. Moreover, $\mathrm{E}[V(Q(t+1)) - V(Q(t))|Q(t) = n] = \mathrm{E}[Q(t+1) - Q(t)|Q(t) = n] = \Delta_n$. In the rest of the Appendix it is shown that $\limsup_{n\to\infty} \Delta_n = \ell < 0$ implies that the two conditions in the statement of Theorem 1 hold.

Let us choose an arbitrary positive ϵ such that $\epsilon < |\ell|$, where $0 > \ell = \limsup_{n\to\infty} \Delta_n$. From $\limsup_{n\to\infty} \Delta_n = \lim_{n\to\infty} \left(\sup_{k\ge n} \Delta_k\right) = \ell$ if follows that there exists N_ϵ such that $|\sup_{k\ge n} \Delta_k - \ell| < |\ell| - \epsilon$, $\forall n > N_\epsilon$. It follows that $\sup_{k\ge n} \Delta_k < \ell + |\ell| - \epsilon = -\epsilon$, $\forall n > N_\epsilon \Rightarrow \Delta_n < -\epsilon$, $\forall n > N_\epsilon$.

On the other hand, $\forall n \le N_\epsilon$ it holds that

$$\begin{aligned}\Delta_n &= \mathrm{E}[A(t)|Q(t) = n] - \mathrm{E}[D(t)|Q(t) = n] \\ &\le \frac{\Lambda L}{W \log_2(1+\gamma_n)} \le \frac{\Lambda L}{W \log_2(1+\gamma_{N_\epsilon})} = b\end{aligned}$$

since γ_n is a non-increasing sequence with n.

Summing up, we have proved that $\Delta_n < -\epsilon$ for any state n, but for a finite set of states, namely for $n \in \{0, 1, \dots, N_\epsilon\}$, for which we have $\Delta_n \le b < \infty$. This completes the proof that the conditions of Foster–Lyapunov theorem are satisfied, if $\limsup_{n\to\infty} \Delta_n < 0$.

Appendix C. Supplementary data

Supplementary material related to this article can be found online at https://doi.org/10.1016/j.peva.2024.102460.

References

[1] X. Chen, D.W.K. Ng, W. Yu, E.G. Larsson, N. Al-Dhahir, R. Schober, Massive access for 5G and beyond, IEEE J. Sel. Areas Commun. 39 (3) (2021) 615–637, http://dx.doi.org/10.1109/JSAC.2020.3019724.

[2] K. Zheng, S. Ou, J. Alonso-Zarate, M. Dohler, F. Liu, H. Zhu, Challenges of massive access in highly dense LTE-advanced networks with machine-to-machine communications, IEEE Wirel. Commun. 21 (3) (2014) 12–18, http://dx.doi.org/10.1109/MWC.2014.6845044.

[3] S.K. Sharma, X. Wang, Toward massive machine type communications in ultra-dense cellular IoT networks: Current issues and machine learning-assisted solutions, IEEE Commun. Surv. Tutor. 22 (1) (2020) 426–471, http://dx.doi.org/10.1109/COMST.2019.2916177.

[4] A. Rajandekar, B. Sikdar, A survey of MAC layer issues and protocols for machine-to-machine communications, IEEE Internet Things J. 2 (2) (2015) 175–186, http://dx.doi.org/10.1109/JIOT.2015.2394438.

[5] L. Liu, E.G. Larsson, W. Yu, P. Popovski, C. Stefanovic, E. de Carvalho, Sparse signal processing for grant-free massive connectivity: A future paradigm for random access protocols in the Internet of Things, IEEE Signal Process. Mag. 35 (5) (2018) 88–99, http://dx.doi.org/10.1109/MSP.2018.2844952.

[6] F. Formaggio, A. Munari, F. Clazzer, On receiver diversity for grant-free based machine type communications, Ad Hoc Netw. 107 (2020) 102245, http://dx.doi.org/10.1016/j.adhoc.2020.102245.

[7] M. Chafii, L. Bariah, S. Muhaidat, M. Debbah, Twelve scientific challenges for 6G: Rethinking the foundations of communications theory, IEEE Commun. Surv. Tutor. 25 (2) (2023) 868–904, http://dx.doi.org/10.1109/COMST.2023.3243918.

[8] Y. Liu, S. Zhang, Z. Ding, R. Schober, N. Al-Dhahir, E. Hossain, X. Shen, Special issue on next generation multiple access—Part I, IEEE J. Sel. Areas Commun. 40 (4) (2022) 1031–1036, http://dx.doi.org/10.1109/JSAC.2021.3139485.

[9] Y. Liu, S. Zhang, X. Mu, Z. Ding, R. Schober, N. Al-Dhahir, E. Hossain, X. Shen, Evolution of NOMA toward next generation multiple access (NGMA) for 6G, IEEE J. Sel. Areas Commun. 40 (4) (2022) 1037–1071, http://dx.doi.org/10.1109/JSAC.2022.3145234.

[10] Y. Mao, O. Dizdar, B. Clerckx, R. Schober, P. Popovski, H.V. Poor, Rate-splitting multiple access: Fundamentals, survey, and future research trends, IEEE Commun. Surv. Tutor. 24 (4) (2022) 2073–2126, http://dx.doi.org/10.1109/COMST.2022.3191937.
[11] J.-B. Seo, B.C. Jung, H. Jin, Performance analysis of NOMA random access, IEEE Commun. Lett. 22 (11) (2018) 2242–2245, http://dx.doi.org/10.1109/LCOMM.2018.2866376.
[12] M.B. Shahab, R. Abbas, M. Shirvanimoghaddam, S.J. Johnson, Grant-free non-orthogonal multiple access for IoT: A survey, IEEE Commun. Surv. Tutor. 22 (3) (2020) 1805–1838, http://dx.doi.org/10.1109/COMST.2020.2996032.
[13] J. Choi, NOMA-based random access with multichannel ALOHA, IEEE J. Sel. Areas Commun. 35 (12) (2017) 2736–2743, http://dx.doi.org/10.1109/JSAC.2017.2766778.
[14] J. Choi, On throughput bounds of NOMA-ALOHA, 2021, CoRR arXiv:2110.12530.
[15] H. Lin, K. Ishibashi, W.-Y. Shin, T. Fujii, A simple random access scheme with multilevel power allocation, IEEE Commun. Lett. 19 (12) (2015) 2118–2121, http://dx.doi.org/10.1109/LCOMM.2015.2489650.
[16] C. Xu, L. Ping, P. Wang, S. Chan, X. Lin, Decentralized power control for random access with successive interference cancellation, IEEE J. Sel. Areas Commun. 31 (11) (2013) 2387–2396, http://dx.doi.org/10.1109/JSAC.2013.131113.
[17] Y. Li, L. Dai, Maximum sum rate of slotted aloha with successive interference cancellation, IEEE Trans. Commun. 66 (11) (2018) 5385–5400, http://dx.doi.org/10.1109/TCOMM.2018.2843338.
[18] A.K. Gupta, T.G. Venkatesh, N. Vuppalapati, SIC and CSI-based random channel access protocol for WLAN supporting multi packet transmission, in: 2022 IEEE Global Conference on Artificial Intelligence and Internet of Things, GCAIoT, 2022, pp. 188–193, http://dx.doi.org/10.1109/GCAIoT57150.2022.10019144.
[19] A.B. Abdul Razzaque, A. Baiocchi, Grant-free transmissions based on successive interference cancellation in IoT, in: 2023 35th International Teletraffic Congress, ITC-35, 2023, pp. 1–9, http://dx.doi.org/10.1109/ITC-3560063.2023.10555710.
[20] A.B. Abdul Razzaque, H.K. Qureshi, A. Baiocchi, Low vs high spectral efficiency communications with SIC and random access, in: 2022 IEEE 11th IFIP International Conference on Performance Evaluation and Modeling in Wireless and Wired Networks, PEMWN, 2022, pp. 1–6, http://dx.doi.org/10.23919/PEMWN56085.2022.9963845.
[21] M. Shirvanimoghaddam, M. Dohler, S.J. Johnson, Massive non-orthogonal multiple access for cellular IoT: Potentials and limitations, IEEE Commun. Mag. 55 (9) (2017) 55–61, http://dx.doi.org/10.1109/MCOM.2017.1600618.
[22] Z. Dawy, W. Saad, A. Ghosh, J.G. Andrews, E. Yaacoub, Toward massive machine type cellular communications, IEEE Wirel. Commun. 24 (1) (2017) 120–128, http://dx.doi.org/10.1109/MWC.2016.1500284WC.
[23] Y. Polyanskiy, A perspective on massive random-access, in: 2017 IEEE International Symposium on Information Theory, ISIT, 2017, pp. 2523–2527, http://dx.doi.org/10.1109/ISIT.2017.8006984.
[24] J. Choi, J. Ding, N.-P. Le, Z. Ding, Grant-free random access in machine-type communication: Approaches and challenges, IEEE Wirel. Commun. 29 (1) (2022) 151–158, http://dx.doi.org/10.1109/MWC.121.2100135.
[25] N.H. Mahmood, R. Abreu, R. Böhnke, M. Schubert, G. Berardinelli, T.H. Jacobsen, Uplink grant-free access solutions for URLLC services in 5G new radio, in: 2019 16th International Symposium on Wireless Communication Systems, ISWCS, 2019, pp. 607–612, http://dx.doi.org/10.1109/ISWCS.2019.8877253.
[26] N.I. Miridakis, D.D. Vergados, A survey on the successive interference cancellation performance for single-antenna and multiple-antenna OFDM systems, IEEE Commun. Surv. Tutor. 15 (1) (2013) 312–335, http://dx.doi.org/10.1109/SURV.2012.030512.00103.
[27] K.R. Patel, S. Dasrao Deshmukh, 2S (superposition coding, successive interference cancellation) operations in NOMA technology for 5G networks: Review and implementation, in: 2023 IEEE 8th International Conference for Convergence in Technology, I2CT, 2023, pp. 1–6, http://dx.doi.org/10.1109/I2CT57861.2023.10126268.
[28] E. Casini, R. De Gaudenzi, O.D.R. Herrero, Contention resolution diversity slotted ALOHA (CRDSA): An enhanced random access schemefor satellite access packet networks, IEEE Trans. Wirel. Commun. 6 (4) (2007) 1408–1419.
[29] J.-L. Lu, W. Shu, M.-Y. Wu, A survey on multi-packet reception for wireless random access networks, J. Comput. Netw. Commun. (2012).
[30] F. Ricciato, P. Castiglione, Pseudo-random aloha for enhanced collision-recovery in RFID, IEEE Commun. Lett. 17 (3) (2013).
[31] M. Ivanov, et al., Broadcast coded slotted ALOHA: A finite frame length analysis, IEEE Trans. Commun. 65 (2) (2017).
[32] G. Liva, Graph-based analysis and optimization of contention resolution diversity slotted ALOHA, IEEE Trans. Commun. 59 (2) (2010) 477–487.
[33] A. Munari, F. Lázaro, G. Durisi, G. Liva, The dynamic behavior of frameless ALOHA: Drift analysis, throughput, and age of information, IEEE Trans. Commun. (2023).
[34] M. Moradian, A. Dadlani, A. Khonsari, H. Tabassum, Age-aware dynamic frame slotted ALOHA for machine-type communications, IEEE Trans. Commun. (2024).
[35] S.A. Tegos, P.D. Diamantoulakis, A.S. Lioumpas, P.G. Sarigiannidis, G.K. Karagiannidis, Slotted ALOHA with NOMA for the next generation IoT, IEEE Trans. Commun. 68 (10) (2020) 6289–6301, http://dx.doi.org/10.1109/TCOMM.2020.3007744.
[36] S.M.R. Islam, N. Avazov, O.A. Dobre, K.-s. Kwak, Power-domain non-orthogonal multiple access (NOMA) in 5G systems: Potentials and challenges, IEEE Commun. Surv. Tutor. 19 (2) (2017) 721–742, http://dx.doi.org/10.1109/COMST.2016.2621116.
[37] S. Sen, N. Santhapuri, R.R. Choudhury, S. Nelakuditi, Successive interference cancellation: Carving out MAC layer opportunities, IEEE Trans. Mob. Comput. 12 (2) (2013) 346–357, http://dx.doi.org/10.1109/TMC.2012.17.
[38] A. Shashin, A. Belogaev, A. Krasilov, E. Khorov, Adaptive parameters selection for uplink grant-free URLLC transmission in 5G systems, Comput. Netw. 222 (2023) 109527, http://dx.doi.org/10.1016/j.comnet.2022.109527.
[39] A. Gizik, O.A. Sensoy, E. Masazade, Enhanced dynamic scheduling for uplink latency reduction in broadband VoLTE systems, in: 2021 55th Asilomar Conference on Signals, Systems, and Computers, 2021, pp. 13–17, http://dx.doi.org/10.1109/IEEECONF53345.2021.9723407.
[40] S.-W. Jeon, H. Jin, Online estimation and adaptation for random access with successive interference cancellation, IEEE Trans. Mob. Comput. 22 (9) (2023) 5418–5433, http://dx.doi.org/10.1109/TMC.2022.3179240.
[41] D.-S. Lee, C.-S. Chang, R. Zhang, M.-P. Lee, Resource allocation for URLLC and eMBB traffic in uplink wireless networks, Perform. Eval. 161 (2023) 102353, http://dx.doi.org/10.1016/j.peva.2023.102353.
[42] P. Brown, S.E. Elayoubi, M. Deghel, A. Galindo-Serrano, Design and performance evaluation of contention-based transmission schemes for URLLC services, Perform. Eval. 143 (2020) 102132, http://dx.doi.org/10.1016/j.peva.2020.102132.
[43] N.V. Matveev, The adaptive retransmission management in random multiple-access system with successive interference cancellation, in: 2018 Wave Electronics and Its Application in Information and Telecommunication Systems, WECONF, 2018, pp. 1–5, http://dx.doi.org/10.1109/WECONF.2018.8604323.
[44] M.M. Ebrahimi, K. Khamforoosh, M. Amini, A. Sheikhahmadi, H. Khamfroush, Adaptive–persistent nonorthogonal random access scheme for URLL massive IoT networks, IEEE Syst. J. 17 (1) (2023) 1660–1671, http://dx.doi.org/10.1109/JSYST.2022.3190132.
[45] B. Razzaque, The role of SIC on the design of next generation multiple access, Ann. Telecommun. (2023) http://dx.doi.org/10.1007/s12243-023-00992-5.
[46] C. Sommer, S. Joerer, F. Dressler, On the applicability of two-ray path loss models for vehicular network simulation, in: 2012 IEEE Vehicular Networking Conference, VNC, 2012, pp. 64–69, http://dx.doi.org/10.1109/VNC.2012.6407446.
[47] F. Clazzer, E. Paolini, I. Mambelli, C. Stefanovic, Irregular repetition slotted ALOHA over the Rayleigh block fading channel with capture, in: 2017 IEEE International Conference on Communications, ICC, 2017, pp. 1–6, http://dx.doi.org/10.1109/ICC.2017.7996796.

[48] C. Stefanovic, D. Vukobratovic, Coded random access, in: Network Coding and Subspace Designs, in: Signals and Communication Technology, Springer, Germany, 2018, pp. 339–359, http://dx.doi.org/10.1007/978-3-319-70293-3-13.
[49] R.D. Yates, Y. Sun, D.R. Brown, S.K. Kaul, E. Modiano, S. Ulukus, Age of information: An introduction and survey, IEEE J. Sel. Areas Commun. 39 (5) (2021) 1183–1210.
[50] D. Bertsekas, R. Gallager, Data Networks, second ed., Prentice-Hall, Inc., USA, 1992.
[51] G. Bianchi, I. Tinnirello, Kalman filter estimation of the number of competing terminals in an IEEE 802.11 network, in: IEEE INFOCOM 2003. Twenty-second Annual Joint Conference of the IEEE Computer and Communications Societies (IEEE Cat. No.03CH37428), vol. 2, 2003, pp. 844–852, http://dx.doi.org/10.1109/INFCOM.2003.1208922.
[52] I. Kadota, A. Baiocchi, A. Anzaloni, Kalman filtering: Estimate of the numbers of active queues in an 802.11e EDCA wlan, Comput. Commun. 39 (2014) 54–64, http://dx.doi.org/10.1016/j.comcom.2013.09.010.
[53] M.J. Neely, Stochastic Network Optimization with Application to Communication and Queueing Systems, Morgan & Claypool, 2010.